Physical Communication 11 (2014) 56–66

Contents lists available at ScienceDirect

Physical Communication

journal homepage: www.elsevier.com/locate/phycom

Full length article

Uplink CFO compensation for FBMC multiple access and OFDMA in a high mobility scenario

Gustavo J. González [a,*], Fernando H. Gregorio [a], Juan Cousseau [a], Risto Wichman [b], Stefan Werner [b]

[a] CONICET-Department of Electrical and Computer Eng., Universidad Nacional del Sur, Av. Alem 1253, Bahía Blanca, 8000, Argentina

[b] Department of Signal Processing and Acoustics, Aalto University School of Electrical Engineering, P.O. Box 13000, 00076 Aalto, Finland

ARTICLE INFO

Article history:
Received 8 February 2013
Received in revised form 31 August 2013
Accepted 4 October 2013
Available online 31 October 2013

Keywords:
OFDMA
FBMC multiple access
Carrier frequency offset
Interference compensation

ABSTRACT

We study in this work CFO compensation methods for two multicarrier multiple access techniques in a high mobility scenario. In particular, we consider orthogonal frequency division multiple access (OFDMA) and filter bank multicarrier multiple access (FBMC-MA). The main motivation for this study is not only the different sensitivity these multicarrier techniques have to CFO but also the different methods they use to reduce CFO effect. In a high mobility scenario the CFO is re-estimated to follow its variation. We show that the frequency at which the CFO is re-estimated has a strong influence in the performance and the complexity of the proposed compensation methods. Additionally, we present a low-complexity CFO compensation method for OFDMA that employs a better approximation of the intercarrier interference than previous approaches. Regarding FBMC-MA, we introduce an extension of a CFO-compensation method that allows to consider a multitap channel equalizer. Finally, using simulations, we compare the performance of the compensation methods over several channel and time-varying CFO conditions.

1. Introduction

Owing to their high data throughput for multimedia applications, spectral efficiency and flexibility, the most promising techniques for the new generation of wireless systems are based on multicarrier modulation schemes. However, the uplink of multicarrier access techniques is highly sensitive to carrier frequency offset (CFO) since it destroys the orthogonality among subcarriers producing intercarrier interference (ICI), and therefore, multiple access interference (MAI) between users. When comparing to downlink synchronization, uplink synchronization is more challenging because each user is characterized by its own particular CFO and channel parameters [1,2].

Uplink frequency synchronization is commonly divided into an acquisition stage followed by a tracking stage. In the acquisition, or coarse estimation, the CFO and the communication channel are estimated using a suitable training sequence at the beginning of each frame [1–3], or through a specific synchronization procedure [4]. In the tracking stage, the estimation of the residual CFO produced by user mobility (Doppler effect) or estimation errors in the acquisition is refined [5]. These estimates are used to compensate the CFO interference.

Even when other alternative schemes for the uplink exist [6], the two options considered in this work are: orthogonal frequency division multiple access (OFDMA) and filter bank multicarrier multiple access (FBMC-MA) [7,8]. FBMC-MA is the multiple access technique based on filter bank multicarrier (FBMC) modulation [9]. The main motivation for this study is not only the different sensitivity these multicarrier techniques have to CFO but also the different form they use to reduce CFO's consequences, considering a high mobility scenario.

* Corresponding author. Tel.: +54 2914595101.
E-mail addresses: ggonzalez@uns.edu.ar (G.J. González), Fernando.gregorio@uns.edu.ar (F.H. Gregorio), jcousseau@uns.edu.ar (J. Cousseau), risto.wichman@aalto.fi (R. Wichman), stefan.werner@aalto.fi (S. Werner).

1874-4907/$ – see front matter © 2013 Elsevier B.V. All rights reserved.
http://dx.doi.org/10.1016/j.phycom.2013.10.002

Some popular approaches for the acquisition stage of uplink CFO compensation in OFDMA use iterative interference cancellation [10,11] or linear suppression [12]. Despite its larger computational complexity, the latter compensation scheme is preferred due to its better bit error rate (BER) performance [13]. Although OFDMA demodulation has low complexity, linear CFO suppression requires the inversion of a huge interference matrix, resulting in a computational complexity that may be prohibitive. A banded approximation of the interference matrix that reduces the matrix inversion complexity at the expense of some residual MAI is proposed in [12].

The FBMC transmission technique can be regarded as an extension of the OFDM concept. The OFDM rectangular time window is replaced by a highly selective filter that, in a multiple access context, leads to a negligible MAI [8]. As a consequence, only intercarrier interference needs to be compensated in FBMC-MA. A low complexity method for CFO compensation in the acquisition stage for FBMC-MA is introduced in [8]. The compensation is equivalent to the post-demodulation compensation for OFDMA, derived in [14], although it performs better due to the lower MAI inherent to FBMC-MA. Even when a low complexity polyphase realization exists [9], the high complexity of the whole FBMC-MA system, i.e. symbol modulation, channel estimation and equalization, and CFO estimation and compensation, is still a problem as discussed in the following sections.

Only a few results are available in the literature considering specifically a high mobility scenario. Blind algorithms for the tracking stage are proposed in [15,16]. A data-aided CFO tracking algorithm is presented in [11], although the CFO compensation procedure does not receive much attention. None of these methods consider a realistic CFO model. In [17] is shown that Rician-fading channels in the mobile context produce time-varying CFO, and a realistic model for this variation is proposed. LTE includes a similar model for the Doppler shift in high speed trains [18, Appendix B].

We study in this work uplink CFO compensation techniques for OFDMA and FBMC-MA systems for the tracking stage. We propose a low complexity alternative for uplink CFO compensation in OFDMA that can be seen as a generalization of the ideas presented in [12]. Comparing with [12], our solution features lower interference for the users at the edges of the band. We also present an algorithm for CFO compensation in FBMC-MA, that includes a multitap channel equalizer. We find that the CFO-compensation technique introduces a phase rotation term that has to be taken into account.

Furthermore, considering a high mobility scenario, we show that the frequency at which the CFO estimation is updated affects the performance and complexity of compensation methods proposed. In our study, we consider separately the operations associated with CFO update and CFO compensation. That allow us to obtain a more realistic complexity measure. To validate the proposed compensation schemes, a detailed simulation study that takes into account several time-varying CFO conditions is included.

The paper is organized as follows. In Section 2 we describe the high mobility scenario and the signal models for OFDMA and FBMC-MA. The CFO compensation schemes for OFDMA and FBMC-MA are derived in Section 3. In Section 4 we present a detailed comparison of the computational complexity for both systems. Numerical simulations and a general discussion are presented in Section 5. Finally, Section 6 concludes the paper.

2. Multicarrier multiple access system model

We consider a centralized system where a base station (BS) controls the information flux from (uplink) and toward (downlink) the users [7,19]. The multicarrier symbol has N subcarriers, where $M < N$ subcarriers are used for data transmission and the remaining $(N - M)$ are virtual subcarriers (VS) located at the edges of the band. Virtual subcarriers avoid frequency leakage to the neighbor bands [7]. Useful subcarriers are divided into K subchannels, where each subchannel containing M/K subcarriers corresponds to a different user. Considering the carrier allocation scheme (CAS), each subchannel is usually composed by an entire number of tiles of size N_t [5]. The tiles of each user can be contiguous to form a subband CAS (SCAS), equispaced to form an interleaved CAS (ICAS), or it can follow a more sophisticated rule, such as maximization of the link quality for every user, to form the generalized CAS (GCAS).

The subcarrier indicator set of each user is $\mathbb{I}^{(k)} = \{\mathbb{I}_0^{(k)} \ldots \mathbb{I}_{N-1}^{(k)}\}$, whose components are defined as

$$\mathbb{I}_m^{(k)} = \begin{cases} 1 & \text{if } m \text{ is allocated to user } k \\ 0 & \text{if } m \text{ is not allocated to user } k \end{cases} \tag{1}$$

where $(\cdot)^{(k)}$ denotes to user k and $0 \leq m \leq N - 1$. The subcarrier indicator sets of different users are disjoint and the union of all sets is complete, i.e. contains the M subcarriers. The components $\mathbb{I}_m^{(k)}$ are defined according to the chosen CAS. The user k transmits symbols

$$X_m^{(k)}(\ell) = \begin{cases} A_m^{(k)}(\ell) & \text{if } \mathbb{I}_m^{(k)} = 1 \\ 0 & \text{otherwise} \end{cases} \tag{2}$$

where $A_m^{(k)}(\ell)$ is a QAM symbol transmitted at subcarrier m, at time ℓ, by user k. We denote the time-varying impulse response of the L-tap wireless channel between user k and the base station as $h_q^{(k)}(n)$, where q is the tap index and n the time index. We also assume that the channel remains constant within a multicarrier symbol (block fading).

2.1. High mobility scenario

Even for a high mobility scenario, the CFO must be below 1% of the intercarrier spacing in order to maintain a negligible degradation [17,20]. We consider two main sources of CFO: user's mobility CFO $\xi_d^{(k)}(\ell)$, related to Doppler effects, and local oscillator drift $\xi_{lo}^{(k)}$.[1] As a consequence, the overall CFO is $\xi^{(k)}(\ell) = \xi_{lo}^{(k)} + \xi_d^{(k)}(\ell)$. Note that in this model the CFO is assumed fixed within a multicarrier symbol and that the CFO terms $\xi_{lo}^{(k)}$ and $\xi_d^{(k)}(\ell)$ are normalized to the intercarrier spacing. During the time

[1] The local oscillator is assumed to have negligible phase noise [21].

required to transmit one frame, $\xi_{lo}^{(k)}$ can be considered as a time-invariant CFO source because it depends on slowly time varying parameters such as temperature, supply voltage, etc. On the other hand, $\xi_d^{(k)}(\ell)$ is time-variant since it depends on the channel characteristics and user mobility [17]. If the users synchronize with the BS in the downlink, the Doppler shift at the BS is doubled, since the displacement that occurs in the downlink is added to the shift in the uplink [19, Section 11]. Local oscillator CFO is compensated in the acquisition stage, whereas Doppler shift is corrected in the tracking stage.

Regarding the magnitude of CFO sources, local oscillators produce a typical variation of ±10 ppm [22]. That variation corresponds to a CFO of 25 kHz for a carrier of 2.5 GHz or 167% of the intercarrier spacing. On the other hand, the maximum Doppler shift for high speed mobiles is several times smaller than that, e.g. for the high speed train scenario [18, Appendix B], with a speed of 350 km/h, the Doppler shift is 1.55 kHz or 10% of the intercarrier spacing.[2] The adverse effects of local oscillator drift and Doppler shift are even worse considering higher carrier frequencies. The trend of increasing the carrier frequency makes the CFO an important issue for next generation systems.

From [17] we know that user mobility CFO is only produced for channels with asymmetric Doppler spectrum. Since Clarke's spectrum does not produce time-varying CFO, to model time variations in $\xi_d^{(k)}(\ell)$ we employ a Rice model, where the line of sight component (LOS) has time varying angle of arrival or velocity. Considering the linear model for CFO variations in [17] and defining tap variances of k user channel as $\{\sigma^2_{h_q^{(k)}}\}_{q=0}^{L-1}$, the average CFO of multicarrier symbol ℓ is given by

$$\xi_d^{(k)}(\ell) = \frac{\sigma^2_{h_0^{(k)}} K_r f_c v^2 T_s^2 N N_m \ell}{(K_r+1) c d_m \sum_{q=0}^{L-1} \sigma^2_{h_q^{(k)}}} \tag{3}$$

where f_c is the carrier frequency, v is the speed of the mobile, T_s is the sampling period, N_m depends on the multicarrier scheme as defined in the next subsections, c the speed of light, d_m is the distance from the base station to the mobile, and K_r is the Rice factor that determines the relation between the power of the LOS component of the first tap and the fading process.

CFO compensation algorithms require the corresponding estimation. For a time-varying CFO, the parameter needs to be re-estimated. The frequency of which the CFO is updated is an important aspect to be considered in the compensation algorithms, since for each new updating instance the CFO interference need to be re-calculated. This issue is addressed in Section 4. Based on previous discussion, CFO requires re-estimation if $|\xi_d^{(k)}(\ell_2) - \xi_d^{(k)}(\ell_1)| > 0.01\Delta f$, where $\xi_d^{(k)}(\ell_1)$ is the CFO due to Doppler of user k at discrete-time ℓ_1 and $\xi_d^{(k)}(\ell_2)$ at ℓ_2, and Δf is intercarrier spacing. We may define $N_u = (\ell_2 - \ell_1)$ as the number of multicarrier symbols under which a CFO estimate is considered valid.

[2] The parameters correspond to 3GPP LTE standard [6].

2.2. OFDMA signal model

Considering perfect time synchronization, the received frequency domain OFDMA signal at the BS, after cyclic prefix (CP) removal can be written as

$$\mathbf{y} = \sum_{k=1}^{K} \mathbf{F}\mathbf{D}^{(k)}\mathbf{F}^{\mathrm{H}}\mathbf{s}^{(k)} + \mathbf{z} \tag{4}$$

where

$$[\mathbf{F}]_{p,q} = \frac{1}{\sqrt{N}} e^{\frac{-j2\pi(p+N_{\mathrm{vs}}-1)(q-1)}{N}}$$

$$\text{for } 1 \le p \le M \text{ and } 1 \le q \le N \tag{5}$$

$$\mathbf{D}^{(k)} = \mathrm{diag}\{1, e^{j2\pi\xi^{(k)}/N}, \ldots, e^{j2\pi\xi^{(k)}(N-1)/N}\} \tag{6}$$

$$\mathbf{s}^{(k)} = [X^{(k)}_{N_{\mathrm{vs}}} H^{(k)}_{N_{\mathrm{vs}}} \ldots X^{(k)}_{N-N_{\mathrm{vs}}-1} H^{(k)}_{N-N_{\mathrm{vs}}-1}]^{\mathrm{T}}. \tag{7}$$

The vector $\mathbf{z}$ is the additive white Gaussian noise (AWGN) at each subcarrier with covariance matrix $\sigma_n^2\mathbf{I}_M$, where $\mathbf{I}_M$ is the $M \times M$ identity matrix. Note that in (4) and (7) the time index ℓ was dropped for simplicity. In the equations, $\mathrm{diag}\{\cdot\}$ denotes the diagonal matrix operator and $N_{\mathrm{vs}} = (N-M)/2$, with $(N-M)$ even, is the number of virtual carriers. The discrete Fourier transform (DFT) of the wireless channel between the user k and the base station at subcarrier m is denoted to as $H_m^{(k)}$. We assume a synchronous system, i.e., that the CP of N_{cp} samples is long enough to accommodate the channel impulse response length and timing misalignments [3]. The OFDMA symbol length with CP is $N_m = N_{\mathrm{cp}} + N$.

The ideal received signal in frequency domain, i.e., without CFO, is given by $\mathbf{s} = \sum_{k=1}^{K} \mathbf{s}^{(k)}$. Considering $\mathbf{s}^{(k)}$, the signal of each user, we can write

$$\mathbf{s}^{(k)} = \mathrm{diag}\{\boldsymbol{\mathcal{I}}^{(k)}\}\mathbf{s}. \tag{8}$$

Replacing (8) in (4) allows us to write the received signal as

$$\mathbf{y} = \boldsymbol{\Pi}\mathbf{s} + \mathbf{z} \tag{9}$$

where

$$\boldsymbol{\Pi} = \sum_{k=1}^{K} \boldsymbol{\Pi}^{(k)} \mathrm{diag}\{\boldsymbol{\mathcal{I}}^{(k)}\} \tag{10}$$

is the overall disturbance, that can be interpreted as an *interference matrix* which relates the orthogonal frequency symbol $\mathbf{s}$, with the actual received symbol in the presence of CFO [12]; and

$$\boldsymbol{\Pi}^{(k)} = \mathbf{F}\mathbf{D}^{(k)}\mathbf{F}^{\mathrm{H}} \tag{11}$$

is the interference matrix of user k. The matrix $\boldsymbol{\Pi}$ is *circulant in blocks*, i.e., the columns that belong to the same user are related by circulant shifts. Note that the interference matrix structure has two components: self-interference and MAI. As shown in the following section, this particular structure can be used to introduce an improved CFO compensation technique for OFDMA.

After CFO compensation, the estimated symbol of all users $\hat{\mathbf{d}}$, can be obtained by

$$\hat{\mathbf{d}} = \mathbf{T}\hat{\mathbf{s}} \tag{12}$$

where $\hat{\mathbf{s}}$ is the CFO-compensated vector, $\mathbf{T} = \mathrm{diag}\{\mathcal{H}^{-1}_{N_{\mathrm{vs}}} \ldots \mathcal{H}^{-1}_{N-N_{\mathrm{vs}}-1}\}$ is the equalization matrix, and $\mathcal{H}_m = H_m^{(k)}$ if $\mathcal{I}_m^{(k)} = 1$.

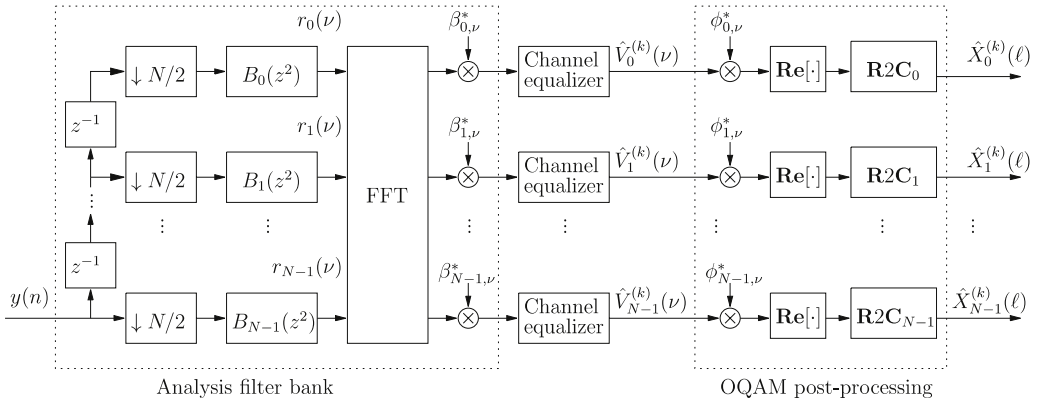

Fig. 1. Block diagram of filter bank multicarrier multiple access demodulation that consists of an analysis filter bank, a channel equalization and a QAM/OQAM transformation.

2.3. FBMC-MA signal model

The received FBMC-MA signal can be described by

$$y(n) = \sum_{k=1}^{K} \left(\sum_{q=0}^{L-1} h_q^{(k)}(n) g^{(k)}(n-q) \right) e^{j2\pi\xi^{(k)}n/N} + w(n) \tag{13}$$

where $g^{(k)}(n)$ are symbols of the kth user, defined in (2), modulated by the synthesis filter bank [23], and $w(n)$ is the additive white Gaussian noise of variance σ_n^2. It is assumed that the timing error is absorbed by the channel model and it is compensated by the channel equalizer [24]. Since no CP is required in FBMC, the multicarrier symbol length is $N_m = N$.

For the analysis filter bank, illustrated in Fig. 1, we have a prototype filter with impulse response $p(n)$ and length $L_{ov}N - 1$, where L_{ov} is the overlapping factor, i.e., the number of FBMC-MA symbols equivalent to the prototype filter length. Also, $\beta_{m,\nu} = (-1)^{m(\nu+L_{ov})}$; $\phi_{m,\nu} = \{1, j, 1, j, \ldots\}$ for m even or $\phi_{m,\nu} = \{j, 1, j, 1, \ldots\}$ for m odd; and $b_m(n) = p(N - 1 - m + nN)$ is the m-th type-2 polyphase component of $p(n)$ with Z-transform $B(z^2)$. Finally, the output vector corresponding to the N branches of the polyphase decomposition at time ν can be described by

$$\mathbf{r}(\nu) = \sum_{q=0}^{L_{ov}-1} \mathbf{r}^{(q)}(\nu) = [r_0(\nu), \ldots, r_{N-1}(\nu)]^{\mathrm{T}}; \tag{14}$$

where

$$\mathbf{r}^{(q)}(\nu) = \mathbf{y}(\nu + 2q) \odot \mathbf{p}(L_{ov} - q),$$
$$\mathbf{y}(\nu) = [y(\nu N/2), \ldots, y(\nu N/2 + N - 1)]^{\mathrm{T}},$$
$$\mathbf{p}(l) = [p(lN), \ldots, p(lN - N + 1)]^{\mathrm{T}} \tag{15}$$

and $\odot$ denotes Hadamard vector product. Considering a multitap equalizer of L_{eq} coefficients, the symbols before the *offset-QAM* (OQAM) post-processing block result

$$\hat{\mathbf{V}}^{(k)}(\nu) = \sum_{l=0}^{L_{eq}-1} \mathbf{G}(\nu - l, \nu) \odot \boldsymbol{\beta}^*(\nu - l) \odot \mathcal{F}\left(\sum_{q=0}^{L_{ov}-1} \mathbf{r}^{(q)}(\nu - l) \right) \tag{16}$$

where $\mathcal{F}\{\cdot\}$ is the FFT operator, $\hat{\mathbf{V}}^{(k)}(\nu) = [\hat{V}_0^{(k)}(\nu) \ldots \hat{V}_{N-1}^{(k)}(\nu)]^{\mathrm{T}}$, $\hat{V}_m^{(k)}(\nu)$ is the output of the channel equalizer, $\boldsymbol{\beta}^*(\nu) = [\beta^*_{0,\nu} \ldots \beta^*_{N-1,\nu}]^{\mathrm{T}}$, $\mathbf{G}(l, \nu) = [\mathcal{E}_0(l, \nu), \ldots, \mathcal{E}_{N-1}(l, \nu)]^{\mathrm{T}}$ and $\mathcal{E}_m(l, \nu)$ is the multitap equalizer impulse response corresponding to time ν, subcarrier m (assigned to user k), for an impulse applied at l [24, Section 4.1]. Note that due to the double sampling frequency of the filter bank, the sampling rate of the channel is also doubled. After CFO compensation and channel equalization, the received OQAM symbols are converted into QAM symbols, as it is illustrated in Fig. 1.

3. Carrier frequency offset compensation

We present in this section the CFO compensation in the tracking stage for the multiple access techniques discussed before, i.e. we assume that the CFO is only produced by the Doppler effect. A generalization of the OFDMA compensation method proposed in [12] is used to obtain a better approximation of the CFO induced interference. In addition, we introduce a CFO compensation method using a popular FBMC-MA implementation with multitap equalization. An estimate of the CFO of each user $\hat{\xi}^{(k)}$ is assumed available.

3.1. OFDMA compensation

To compensate CFO effects in the received multiuser symbol, we need to estimate $\mathbf{s}$ from

$$\mathbf{y} = \boldsymbol{\Pi}\mathbf{s} + \mathbf{z}. \tag{17}$$

We may consider two estimation methods to recover $\mathbf{s}$ [25]. The first one is the least squares (LS) estimate, and is given by

$$\hat{\mathbf{s}}_{\mathrm{LS}} = (\boldsymbol{\Pi}^{\mathrm{H}}\boldsymbol{\Pi})^{-1}\boldsymbol{\Pi}^{\mathrm{H}}\mathbf{y} = \boldsymbol{\Pi}^{-1}\mathbf{y} \tag{18}$$

where the right hand side of this equation is valid only if $\boldsymbol{\Pi}$ is full rank and square [12]. The second method is the minimum mean square error (MMSE), and given by

$$\hat{\mathbf{s}}_{\mathrm{MMSE}} = \mathbf{R}\boldsymbol{\Pi}^{\mathrm{H}}(\boldsymbol{\Pi}\mathbf{R}\boldsymbol{\Pi}^{\mathrm{H}} + \sigma_n^2\mathbf{I}_M)^{-1}\mathbf{y} = \boldsymbol{\Pi}^{\mathrm{H}}\left(\boldsymbol{\Pi}\boldsymbol{\Pi}^{\mathrm{H}} + \frac{\sigma_n^2}{\sigma_s^2}\mathbf{I}_M\right)^{-1}\mathbf{y} \tag{19}$$

where $\mathbf{R} = \mathrm{E}\{\mathbf{s}\mathbf{s}^{\mathrm{H}}\}$ and $\mathrm{E}\{\cdot\}$ is the expectation operator. In the second term it is assumed an identical average power

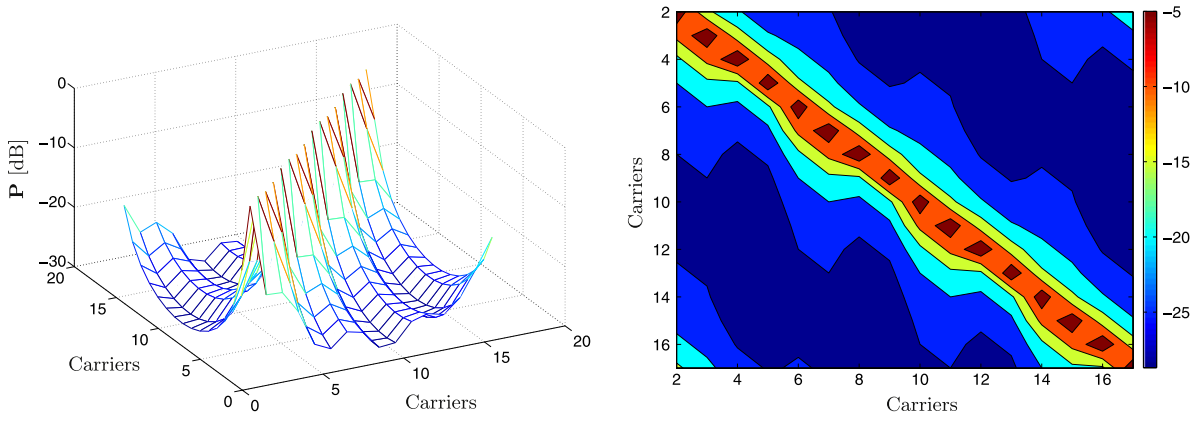

(a) Surface plot. (b) Contour plot.

Fig. 2. CFO-interference power for an OFDMA system with $N = 16$ subcarriers, $K = 2$ users, tile size $N_t = 2$, $\xi^{(1)} = 0.2$ and $\xi^{(2)} = -0.3$, and interleaved CAS. Fig. 2(b) shows the contour plot and Fig. 2(a) illustrates the surface plot.

over all subcarriers σ_s^2, i.e. $\mathbf{R} = \sigma_s^2 \mathbf{I}_M$. As seen above, both methods require the inversion of the interference matrix given in (10), resulting in a high computational burden. We denote these methods as *complete* compensation.

In the following we show that the structure of the interference matrix can be exploited to obtain an efficient approximated solution for the CFO compensation problem. The interference of each user is described by $\mathbf{\Pi}^{(k)}$ in (11), and depends on the CFO of user k. The elements of this matrix are given by [11]

$$[\mathbf{\Pi}^{(k)}]_{p,q} = \frac{1}{N} \frac{1 - e^{j2\pi(q-p+\hat{\xi}^{(k)})}}{1 - e^{j2\pi(q-p+\hat{\xi}^{(k)})/N}} \tag{20}$$

for $1 \leq p, q \leq M$. As noted from (10), the qth column of $\mathbf{\Pi}$ is the qth column of $\mathbf{\Pi}^{(k)}$, if $\mathcal{I}_q^{(k)} = 1$.

Fig. 2 depicts the interference power matrix expressed in dB, with elements given by $[\mathbf{P}]_{p,q} = 20 \log_{10}(|[\mathbf{\Pi}]_{p,q}|)$. This example corresponds to a system with $N = 16$ subcarriers, without virtual subcarriers, two users ($K = 2$) with $\xi^{(1)} = 0.2$ and $\xi^{(2)} = -0.3$, tile size $N_t = 2$ and ICAS. User 1 is assigned to odd tiles and user 2 to even tiles. Fig. 2(a) illustrates the surface plot, whereas Fig. 2(b) shows the contour plot. The terms $[\mathbf{\Pi}]_{p,q}$, describe the interference that the qth subcarrier of the transmitted OFDMA symbol causes to the pth subcarrier of the received symbol. Specifically, we note the following from the figure:

- The power of the interference is concentrated for values of $|q - p|$ close to 0 or N, as it is seen in Fig. 2(a).
- The periodic structure of (20) makes that columns of $\mathbf{\Pi}$ are related by circular shifts, as long as they belong to the same user. This symmetry condition is noted in Fig. 2(b).
- Discontinuities in the columns of $\mathbf{\Pi}$ are due to the different CFO of each user. This can be seen in the pattern of the diagonal terms, shown in Fig. 2(b).

Given the block circular symmetry of the $\mathbf{\Pi}$ matrix and considering the position of the main interference terms, we propose the circular banded compensation (CBC) method depicted in Fig. 3, that is an approximation of the interference matrix $\mathbf{\Pi}$ with *cyclic band structure*. The matrix *bandwidth* τ controls the compensation capability and $\tau_2 = \tau - 2N_{\text{vs}}$. The matrix approximation is defined by

$$[\mathbf{\Pi}_{\text{CB}}]_{p,q} = \begin{cases} [\mathbf{\Pi}]_{p,q} & \text{if } |q-p| \leq \tau \\ [\mathbf{\Pi}]_{p,q} & \text{if } N - \tau \leq |q-p| \\ & \leq M - 1 \text{ and } \tau \geq 2N_{\text{vs}} + 1 \\ 0 & \text{otherwise.} \end{cases} \tag{21}$$

From (21) we see that $M - 1 - (N - \tau) \geq 0$, which means $\tau \geq 2N_{\text{vs}} + 1$, since $N = M + 2N_{\text{vs}}$. As the τ value increases, the interference is reduced at expense of increasing the complexity. This approximation allows to reduce significantly the complexity for computing $\hat{\mathbf{s}}$.

Using (21) in either (18) or (19) lead to CBC-based LS method or CBC-based MMSE method, which requires the inversion of $\mathbf{\Pi}_{\text{CB}}$. By exploiting the banded matrix structure and the fact that most of the matrix components are zero, it is possible to derive low complexity algorithms for the inversion of $\mathbf{\Pi}_{\text{CB}}$. These efficient algorithms can use, for example, LU decomposition and backward and forward substitution [26]. The approximation in (21) allows a trade off between complexity and interference cancellation.

For the case when $\tau \leq 2N_{\text{vs}}$, the terms outside the main diagonal are masked by the VS. Then, the circular banded compensation coincides with the banded compensation (BC) proposed in [12]. However, whenever $\tau \geq 2N_{\text{vs}} + 1$, the BC technique neglects significant interference terms, defined by $N - \tau \leq |q - p| \leq M - 1$ in (21), resulting in a considerable performance degradation when compared to our approach. We shall see that, at the cost of moderate increase in complexity, CBC outperforms BC specially for subcarriers at the edges of the band. In Section 4 we evaluate the computational complexity of CBC and BC for LS and MMSE methods, considering a time-varying scenario.

Regarding OFDMA BER performance considering different CAS, it is reasonable to assume that, due to the frequency diversity introduced, ICAS outperforms SCAS. However, ICAS also increases the MAI generated by the CFO if an approximated compensation is employed. An interpretation of that MAI increment is the increase in the number of transitions between the group of subcarriers (tiles) corresponding to each user. As a consequence, it is not assumed that either CAS leads to specific performance advantage.

3.2. FBMC-MA compensation

The FBMC-MA prototype filter $p(n)$, is designed to have low sidelobes to limit the intercarrier interference to a few subcarriers. For the special case of SCAS no multiple-access interference cancellation is required if a few guard subcarriers are inserted between users . Therefore, the only intercarrier interference is the self-interference of each user. The direct cancellation method proposed in [14] can be used to eliminate the intercarrier interference of each user in the FBMC scheme of [9]. The intercarrier interference compensation is performed by counter-rotating the input to the receiver at the angular frequency given by the user's estimated CFO. That is, by replacing the input signal $y(n)$ by $y(n)e^{-j2\pi\hat{\xi}^{(k)}n/N}$ in (15), where $\hat{\xi}^{(k)}$ denotes the CFO estimate of user k, we obtain the compensation of $\mathbf{r}^{(q)}(\nu)$, as given by

$$\bar{\mathbf{r}}^{(q)}(\nu) = e^{-j\pi\hat{\xi}^{(k)}\nu}e^{-j2\pi\hat{\xi}^{(k)}q}\mathbf{c}(\hat{\xi}^{(k)}) \odot \mathbf{r}^{(q)}(\nu) \tag{22}$$

where $\mathbf{c}(\hat{\xi}^{(k)}) = [1\ e^{-j2\pi\hat{\xi}^{(k)}/N} \ldots e^{-j2\pi\hat{\xi}^{(k)}(N-1)/N}]^{\mathrm{T}}$.

By inserting $\bar{\mathbf{r}}^{(q)}(\nu)$ in (16) we obtain

$$\hat{\mathbf{V}}^{(k)}(\nu) = e^{-j\pi\hat{\xi}^{(k)}\nu}\left(\sum_{l=0}^{L_{\mathrm{eq}}-1}\mathbf{G}(\nu-l,\nu)e^{j\pi\hat{\xi}^{(k)}l} \odot \boldsymbol{\beta}^*(\nu-l) \odot \mathcal{F}\left\{\sum_{q=0}^{L_{\mathrm{ov}}-1} e^{-j2\pi\hat{\xi}^{(k)}q}\mathbf{c}(\hat{\xi}^{(k)}) \odot \mathbf{r}^{(q)}(\nu-l)\right\}\right). \tag{23}$$

Note that the CFO introduces the phase term $e^{j\pi\hat{\xi}^{(k)}l}$, that must be taken into account in the structure of the multitap equalizer shown in (23).

Eq. (23) requires a large amount of calculations to remove the CFO interference of every user. Employing the replication identity defined by

$$\begin{aligned}\psi(n) &= \sum_{q=0}^{L_{\mathrm{ov}}-1}\gamma(n-qN) \longleftrightarrow \Psi(k)\\ &= \Gamma(kL_{\mathrm{ov}}) = \lfloor\Gamma(k)\rfloor_{\downarrow L_{\mathrm{ov}}}\end{aligned} \tag{24}$$

where $\gamma(n)$ and $\psi(n)$ are signals of length NL_{ov} and N, respectively, and $\Gamma(k)$, $\Psi(k)$ are the DFTs of $\gamma(n)$ and $\psi(n)$, it is possible to derive a simplified expression that significantly reduces the complexity. Then, by defining

$$\begin{aligned}\mathbf{c}'(\hat{\xi}^{(k)}) &= [\mathbf{c}^{\mathrm{T}}(\hat{\xi}^{(k)}), e^{-j2\pi\hat{\xi}^{(k)}}\mathbf{c}^{\mathrm{T}}(\hat{\xi}^{(k)}), \ldots,\\ &\quad e^{-j2\pi\hat{\xi}^{(k)}(L_{\mathrm{ov}}-1)}\mathbf{c}^{\mathrm{T}}(\hat{\xi}^{(k)})]^{\mathrm{T}}, \quad \text{and}\\ \mathbf{r}'(\nu) &= [(\mathbf{r}^{(0)})^{\mathrm{T}}, \ldots, (\mathbf{r}^{(L_{\mathrm{ov}}-1)})^{\mathrm{T}}]^{\mathrm{T}},\end{aligned}$$

the compensated OQAM symbols can be written as

$$\begin{aligned}\hat{\mathbf{V}}^{(k)}(\nu) &= e^{-j\pi\hat{\xi}^{(k)}\nu}\left(\sum_{l=0}^{L_{\mathrm{eq}}-1}\mathbf{G}(\nu-l,\nu)e^{j\pi\hat{\xi}^{(k)}l} \odot \boldsymbol{\beta}^*(\nu-l) \odot \left\lfloor\mathcal{F}\left\{\mathbf{c}'(\hat{\xi}^{(k)}) \odot \mathbf{r}'(\nu-l)\right\}\right\rfloor_{\downarrow L_{\mathrm{ov}}}\right)\\ &= e^{-j\pi\hat{\xi}^{(k)}\nu}\left(\sum_{l=0}^{L_{\mathrm{eq}}-1}\mathbf{G}(\nu-l,\nu)e^{j\pi\hat{\xi}^{(k)}l} \odot \boldsymbol{\beta}^*(\nu-l) \odot \left\lfloor\mathcal{F}\left\{\mathbf{c}'(\hat{\xi}^{(k)})\right\} \circledast \mathcal{F}\left\{\mathbf{r}'(\nu-l)\right\}\right\rfloor_{\downarrow L_{\mathrm{ov}}}\right)\end{aligned} \tag{25}$$

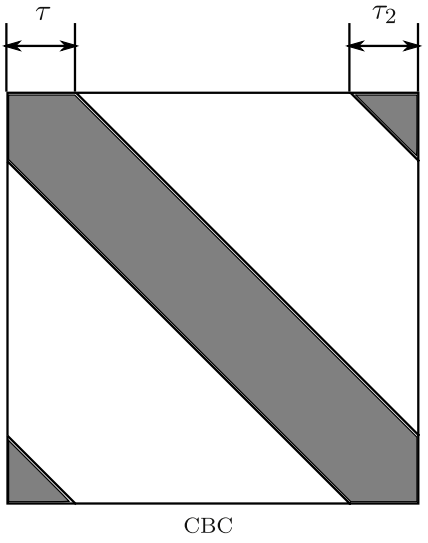

Fig. 3. Structure of the proposed CBC matrix $\mathbf{\Pi}_{\mathrm{CB}}$. Gray elements denote non-zero values.

where $\circledast$ is the circular convolution and the FFTs has length $L_{\mathrm{ov}}N$. As a small number of components of $\mathcal{F}\left\{\mathbf{c}'(\hat{\xi}^{(k)})\right\}$ have significant values, to reduce the complexity we consider only the highest L_{cfo} and set the other to zero [8]. For one-tap equalization, the following compensation of the OQAM symbols results

$$\begin{aligned}\hat{\mathbf{V}}^{(k)}(\nu) &= e^{-j\pi\hat{\xi}^{(k)}\nu}\mathbf{G}(\nu) \odot \boldsymbol{\beta}^*(\nu)\\ &\quad \odot \left\lfloor\mathcal{F}\left\{\mathbf{c}'(\hat{\xi}^{(k)})\right\} \circledast \mathcal{F}\left\{\mathbf{r}'(\nu)\right\}\right\rfloor_{\downarrow L_{\mathrm{ov}}}\end{aligned} \tag{26}$$

where $\mathbf{G}(\nu) = [\mathcal{H}_0^{-1}(\nu), \ldots, \mathcal{H}_{N-1}^{-1}(\nu)]^{\mathrm{T}}$ and $\mathcal{H}_m(\nu)$ is the channel frequency response corresponding to user k, subcarrier m and time ν, if $\mathbb{1}_m^{(k)} = 1$. A similar CFO compensation method is proposed in [8] for one-tap equalization and a different FBMC-MA realization [27]. Note that the CFO-induced phase term in the multitap equalizer of (23) does not appear in the one-tap equalizer of (26).

An additional comment related to FBMC-MA BER performance is important at this point. Different to the case of OFDMA, ICAS or GCAS cannot be employed for FBMC-MA since affordable solutions of low complexity are not available. Despite of that, FBMC-MA reduces MAI that leads to a low performance degradation due to CFO.

If the CFO update is not required for every symbol, the resulting complexity is lower since it is not necessary to update the LU decomposition of matrix $\mathbf{\Pi}_{\mathrm{CB}}$ in (18) and (19), and re-calculate vector $\mathcal{F}\left\{\mathbf{c}'(\hat{\xi}^{(k)})\right\}$ in (26). In the next section we study the computational complexity of the OFDMA and FBMC-MA receivers.

4. Complexity comparison

In this section we focus on the number of real multiplications involved in the implementation of the multicarrier schemes discussed previously. First we derive the complexity of CFO compensation techniques, and then we

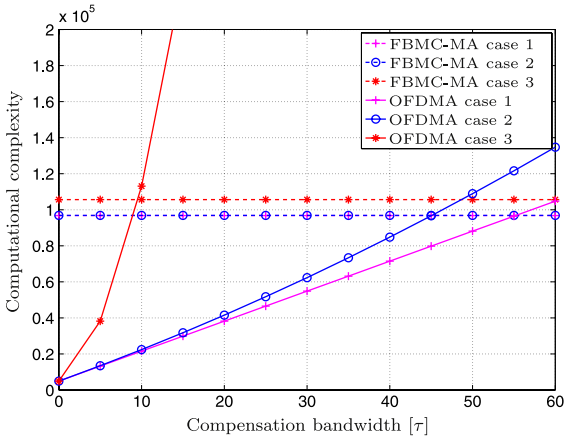

Fig. 4. Computational complexity of multicarrier receivers versus interference bandwidth τ for three cases of CFO: time invariant (case 1), slowly time-variant CFO (case 2), and highly time-variant (case 3).

obtain the complexity of the complete receiver. A complex multiplication is assumed equivalent to four real multiplications and the FFT/IFFT is implemented with the radix-2 algorithm. We show that if the CFO value is not updated for each multicarrier symbol, the complexity of the compensation schemes can be reduced considerably. For this complexity analysis is useful to separate CFO update from CFO compensation operations.

For CFO compensation in OFDMA, we consider the cases of a CFO interference matrix $\mathbf{\Pi}$ with complete, banded and circular banded interference structure. The LS compensation method can be calculated in three steps: (1) LU factorization of $\mathbf{\Pi}$, (2) forward substitution, and (3) backward substitution. On the other hand, the procedure for MMSE compensation is formed by: (1) obtain $\mathbf{Q} = \mathbf{\Pi}\mathbf{\Pi}^{\mathrm{H}} + \sigma_n^2/\sigma_s^2\mathbf{I}$, where $\mathbf{Q}$ is banded or circular banded with double bandwidth if $\mathbf{\Pi}$ is banded or circular banded, (2) LU factorization of $\mathbf{Q}$, (3) forward substitution, (4) backward substitution, and (5) multiplication by matrix $\mathbf{\Pi}^{\mathrm{H}}$. Table 1 summarizes the computational complexity of CFO compensation algorithms, where CFO update and CFO compensation operations are shown separately. Note that $\mu = 2\tau - 2N_{\mathrm{vs}}$ for CBC. The complexity of the CFO update is given by step (1) of LS criterion and steps (1) and (2) of MMSE criterion, whereas the complexity of CFO compensation is given by step (3) of LS criterion, and steps (3)–(5) of MMSE criterion. The CFO compensation complexity for FBMC-MA can be obtained from (25), where again it is considered separately the CFO update and CFO compensation operations. CFO update requires L_{cfo} samples of a NL_{ov}-point FFT, which amounts $2NL_{\mathrm{ov}}\log_2(L_{\mathrm{cfo}})$ multiplications, whereas CFO compensation is a circular convolution that demands $8NL_{\mathrm{cfo}}$ operations [8].

Table 2 summarizes the number of operations required for the implementation of an FBMC-MA or OFDMA receiver. The table breaks up the computational complexity along its different sources, which allows us to do a detailed analysis. The *demodulation* process considers for the FBMC-MA case the number of operations of filter bank branches, the NL_{ov}-point FFT, and phase rotations, whereas for OFDMA it considers an N-point FFT. The table also includes

Table 1
Number of real multiplications for complete, BC, and CBC compensation methods for OFDMA (M: number of used subcarriers, τ: interference matrix bandwidth parameter, $\mu = 2\tau - 2N_{\mathrm{vs}}$).

Compensation	CFO update	CFO compensation
Complete (LS)	$8/3M^3$	$16M^2$
Complete (MMSE)	$32/3M^3$	$16M^2$
BC (LS)	$4M(\tau^2+\tau)$	$8M\tau$
BC (MMSE)	$4M(5\tau^2+4\tau)$	$16M\tau$
CBC (LS)	$4M(\mu^2+\mu)$	$8M\mu$
CBC (MMSE)	$4M(8\mu^2+(2\tau+1)^2+2\mu)$	$8M(2\mu+\tau)$

the complexity of the CFO update, CFO compensation, and channel equalization operations. For CFO compensation in OFDMA the simplified interference matrix with the CBC approach is used. LS is simpler than MMSE and results in the same performance for mid-to-high SNR regime, that are the SNRs of interest. Therefore we consider only LS in our application. From the table we see that the main complexity sources are:

- FBMC-MA: the NL_{ov}-size FFTs and the CFO compensation, calculated for *each received symbol*.
- OFDMA: the inversion of the CFO interference matrix, required for *every new CFO estimation*.

As a direct consequence, if the CFO is required to be re-estimated too often the overall complexity of the OFDMA compensation results very high. In the following, we compare the complexity of complete OFDMA and FBMC-MA receivers for three different CFO update rates.

Case 1 *Time-invariant CFO*: With a constant CFO the update is not required, giving the lower-bound in terms of implementation complexity. The operations for FBMC-MA are: $8NL_{\mathrm{ov}} + 4NL_{\mathrm{ov}}\log_2(NL_{\mathrm{ov}}) + 8M + 8NL_{\mathrm{cfo}} + 8ML_{\mathrm{eq}}$, whereas for the case of OFDMA we have: $2N\log_2(N) + 8M\mu + 4M$.

Case 2 *Slowly time-variant CFO*: The CFO is updated every N_u multicarrier symbols. Then, the multiplications involved in CFO update are divided by the update period N_u. Regarding FBMC-MA, we have $8NL_{\mathrm{ov}} + 4NL_{\mathrm{ov}}\log_2(NL_{\mathrm{ov}}) + 8M + 8NL_{\mathrm{cfo}} + \frac{2NL_{\mathrm{ov}}}{N_u}\log_2(L_{\mathrm{cfo}}) + 8ML_{\mathrm{eq}}$ and for OFDMA results in $2N\log_2(N) + 8M\mu + 4M + \frac{4M}{N_u}(\mu^2+\mu)$.

Case 3 *Highly time-variant CFO*: The CFO is updated every symbol, and it can be considered as the worst case of the OFDMA implementation complexity. The operations for FBMC-MA are $8NL_{\mathrm{ov}} + 4NL_{\mathrm{ov}}\log_2(NL_{\mathrm{ov}}) + 8M + 8NL_{\mathrm{cfo}} + 2NL_{\mathrm{ov}}\log_2(L_{\mathrm{cfo}}) + 8ML_{\mathrm{eq}}$ and for OFDMA we have $2N\log_2(N) + 8M\mu + 4M + 4M(\mu^2+\mu)$ real multiplications.

Fig. 4 illustrates how the computational complexity of both systems varies as a function of the compensation bandwidth τ for the three cases outlined above. The length of FBMC-MA equalizer is $L_{\mathrm{eq}} = 3$ and for the Case 2, $N_u = 200$. Considering Case 1, OFDMA has lower complexity than FBMC-MA for $\tau < 55$. For Case 2, $\tau < 45$ is required to have an OFDMA system with lower complexity than FBMC-MA. Finally, for Case 3, OFDMA is the less complex option if $\tau < 9$. In Section 5 we compare the bit error rate performance of both systems considering different compensation bandwidths to show the tradeoff between complexity and bit error rate (BER) for different update rates.

Table 2
Demodulation, CFO compensation, CFO update, and channel equalization (CE) implementation complexities in FBMC-MA and OFDMA receivers. (N: total number of subcarriers, M: number of used subcarriers, $\mu = 2\tau - 2N_{vs}$, L_{ov}: overlapping factor, L_{cfo}: terms of reduced CFO compensation [8], L_{eq}: equalizer length.)

Scheme	Demodulation	CFO compensation	CFO update	CE
FBMC-MA	$8NL_{ov} + 4NL_{ov}\log_2(NL_{ov}) + 8M$	$8NL_{cfo}$	$2NL_{ov}\log_2(L_{cfo})$	$8ML_{eq}$
OFDMA	$2N\log_2(N)$	$8M\mu$	$4M(\mu^2+\mu)$	$4M$

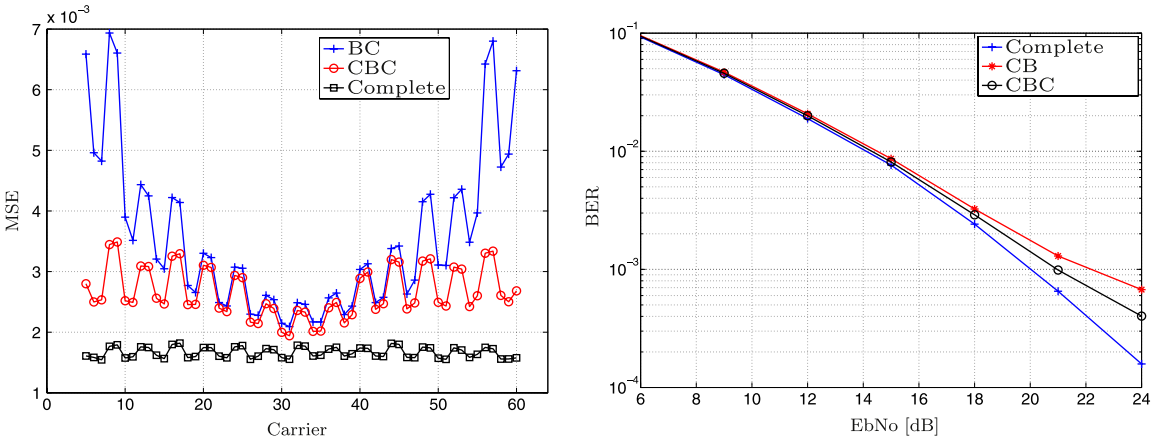

(a) MSE vs. Carrier.

(b) BER of a user allocated at the edge of the band.

Fig. 5. Performance of CFO compensation in OFDMA employing: BC, CBC and complete interference matrix approaches. Fig. 5(a) shows the mean square error versus carrier index, whereas Fig. 5(b) illustrates the BER of a user allocated at the edge of the band.

5. Simulations and discussion

In this section, we illustrate the performance of the schemes discussed in previous sections. We first evaluate the mean square error (MSE) and bit error rate (BER) of CFO compensation in OFDMA considering CBC, BC [12] and the complete interference matrix $\mathbf{\Pi}$. Then we simulate the performance of OFDMA and FBMC-MA CFO compensation for fixed CFO, i.e. without Doppler shift. The objective is to study the performance of the compensation independently of the CFO estimation stage, i.e. assuming that the CFO is known in the receiver. Then, we verify the robustness of the compensation techniques against CFO estimation errors. Finally, we compare OFDMA and FBMC-MA CFO for a time-varying CFO to put particular emphasis to the high mobility scenario.

The comparison between CBC, BC and complete interference matrix $\mathbf{\Pi}$ for CFO compensation in OFDMA is depicted in Fig. 5. Note that FBMC-MA compensation algorithm is not included since its performance does not depend on the carrier index. The system parameters are: total number of subcarriers $N = 64$, used subcarriers $M = 56$, the cyclic prefix length $N_{cp} = 16$, the number of subcarriers of the tile $N_t = 4$, the number of users $K = 2$, the bandwidth compensation parameter $\tau = 25$, interleaved CAS, and the CFO is taken as a random variable uniformly distributed in the range $|\xi^{(k)}| < 0.3$. The MSE defined as $\text{MSE} = \text{E}\{\|(\hat{\mathbf{s}} - \mathbf{s})\|^2\}$ is shown in Fig. 5(a) for an SNR of 30 dB. We consider an AWGN channel to not mask the CFO compensation pattern. We see that in the CBC approach the performance is better than the BC approach at the edges of the band. The reason for this performance improvement is the use of the *cyclic band structure* of the interference matrix, defined in Section 3.1. The approximate complexity of CBC in terms of real multiplications is 420E+3 operations. Complete compensation and BC are included as a benchmark and require 520E+3 and 170E+3 real multiplications, respectively. From Fig. 5(a) we see that subcarriers allocated at the edges of the transmission band suffer more interference for approximate algorithms. The effect of this residual interference is illustrated in Fig. 5(b), where we plot the BER of a user with subcarriers allocated at the edge of the band considering the Vehicular A propagation channel [28] and perfect time synchronization. The figure shows that the CBC increases the performance of this user compared with BC approach.

For BER simulations we use a coded 3GPP LTE - like system with the following parameters: a total number of subcarriers $N = 1024$, transmission bandwidth $BW = 20$ MHz, and carrier frequency $f_c = 2.5$ GHz. We consider four users ($K = 4$), 1/2-rate code [133_8, 177_8] and 16-QAM modulation. Each user transmits data in a burst of contiguous multicarrier blocks. OFDMA has a cyclic prefix of $N_{cp} = 112$, a tile size of 5 subcarriers and 41 tiles per user for ICAS, and 205 subcarriers per user for SCAS. The basic parameters for FBMC-MA are $L_{ov} = 4$, one guard carrier and 205 subcarriers per user. The prototype filter is designed using the frequency sampling technique [23] and a multitap equalizer with $L_{eq} = 3$ is adopted [24, Section 4.1]. We assume perfect time synchronization and that the channel is known at the receiver. The results are averaged over 40 user allocations and 40 noise realizations for each specified SNR.

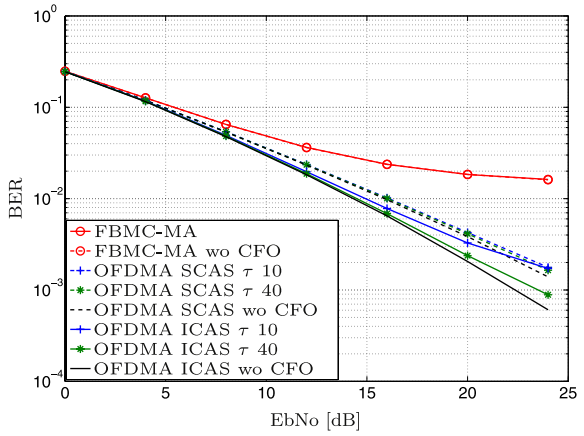

(a) Low CFO.

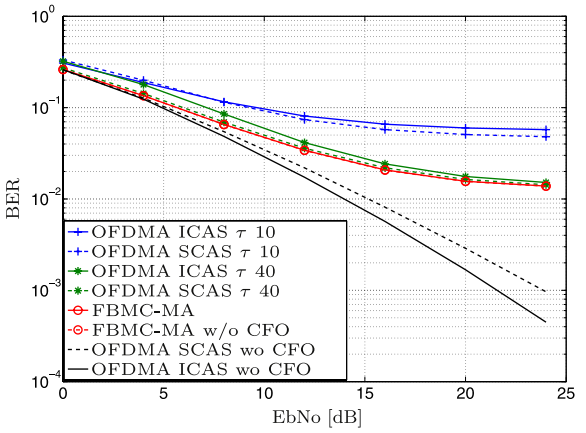

(b) High CFO.

Fig. 6. OFDMA and FBMC-MA CFO compensation schemes for fixed CFO considering the Vehicular A channel. In Fig. 6(a) is considered low CFO ($|\xi^{(k)}| < 0.1$) whereas in Fig. 6(b) high CFO ($|\xi^{(k)}| < 0.5$).

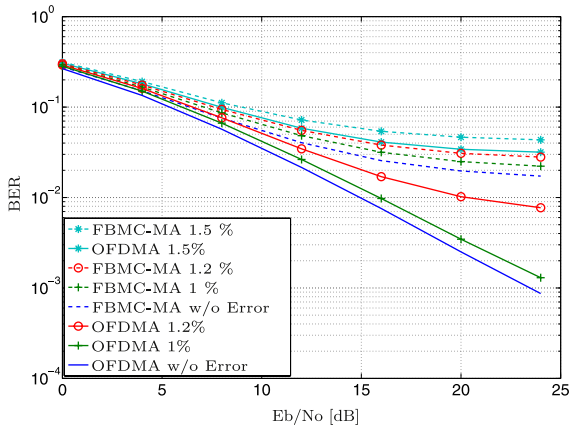

Fig. 7. Performance of OFDMA and FBMC-MA CFO compensation schemes considering errors in the estimation of the CFO value.

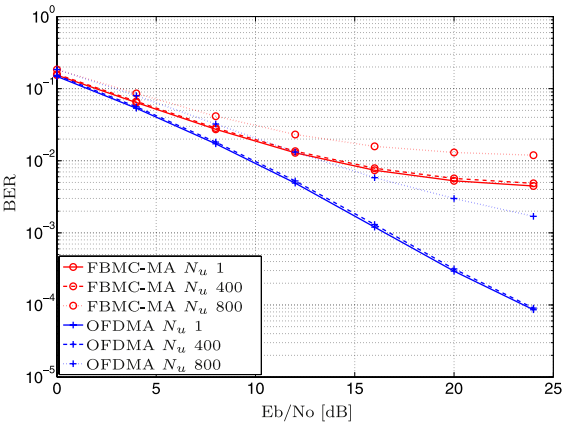

Fig. 8. OFDMA and FBMC-MA CFO compensation schemes for time-variant CFO considering the Rician channel in [17]. The CFO value is updated every $N_u = 1$, $N_u = 400$ and $N_u = 800$ multicarrier symbols.

Fig. 6 illustrates the performance of OFDMA and FBMC-MA CFO compensation schemes for the Vehicular A propagation channel [28] with a speed of 100 km/h. We consider an invariant CFO uniformly distributed. ICAS and SCAS are included for OFDMA, whereas FBMC-MA is constrained to have SCAS. In Fig. 6(a) we consider low CFO values ($|\xi^{(k)}| < 0.1$) whereas in Fig. 6(b) high values ($|\xi^{(k)}| < 0.5$). From Fig. 6(a), we note that for low CFO OFDMA outperform FBMC both in BER and complexity regardless the chosen CAS (see Fig. 4). On the other hand, Fig. 6(b) shows that FBMC-MA has better performance than OFDMA for high CFO, except for $\tau = 40$ where the performance is similar. Using the compensation technique proposed for OFDMA, ICAS introduces frequency diversity but at the same time increases the MAI, as introduced in Section 3.1. As a consequence for low CFO, and therefore low MAI, ICAS has better performance than SCAS since diversity prevails. On the other hand, for high CFO SCAS is the best option due to the notorious increase of MAI. FBMC-MA is not affected by the increase of CFO value since it has not MAI, as is described in Section 3.2. Therefore, FBMC-MA admits higher carrier frequencies and lower quality local oscillators than OFDMA. The BER floor observed in FBMC-MA is a consequence of the lack of robustness against channel variations. Since FBMC-MA does not employ a cyclic prefix (CP), it suffers from inter-symbol interference (ISI) if the channel is time variant. FBMC-MA equalization reduces the intercarrier (ICI) interference, but not the inter-symbol interference (ISI). Then, for time-varying channels the performance of the FBMC-MA system is degraded.

The effect of CFO estimation errors in the BER performance of proposed algorithms is depicted in Fig. 7. The CFO estimation error of ε% is defined as $\hat{\xi}^{(k)} = (1 + \varepsilon/100)\xi^{(k)}$. The figure shows that the performance of both systems is affected by CFO estimation errors but OFDMA is clearly more robust than FBMC-MA to errors in the CFO estimation. For example, considering a BER of 3×10^{-2} and 1% of CFO estimation error, OFDMA requires 0.8 dB extra whereas FBMC-MA 2.5 dB.

Fig. 8 illustrates the performance of time-varying CFO compensation in OFDMA and FBMC-MA systems, for different CFO update periods N_u and subband CAS. Following the Rician-fading model in [17], the time-varying CFO is obtained from (3) considering $K_r = 15$, $v = 100$ km/h, and $d_m = 50$ m. The channel has an exponential decay profile given by $\sigma^2_{h_q} = \exp(-9.2qT_s/1\,\mu s)$ with $0 \leq q \leq L-1$, $L = 5$. From Fig. 8 we see that OFDMA is more robust to long CFO re-estimation periods, i.e., to higher N_u values. Despite the variations in the CFO are considerable due to the high mobility assumption, long update periods (e.g. $N_u = 400$) are feasible. As a consequence, the solution presented in Case 2 of Section 4 leads to a considerable complexity reduction. A recent test bench for high speed trains was proposed in [18, Appendix B], where $v = 350$ km/h and $d_m = 50$ m. Considering $f_c = 2.5$ GHz, $\Delta f = 15$ kHz [6], and a Doppler drift of 1% of Δf, the CFO needs to be re-estimated every $N_u \approx 1140$ multicarrier symbols or 190 subframes. This agrees with the results obtained in Figs. 7 and 8.

6. Conclusion

In this work we study orthogonal frequency division multiple access (OFDMA) and filter bank multicarrier multiple access (FBMC-MA) as modulation schemes for the uplink of multiuser communication systems with carrier frequency offset (CFO). We propose a novel approximation to the interference generated by the CFO in OFDMA. Our proposal is able to reduce the multiple access interference and has lower interference for users allocated at the edges of the band. For the case of FBMC-MA, we propose a CFO compensation considering multitap channel equalization. Considering a time-varying CFO, we find that the complexity of OFDMA is due to the frequency at which the CFO is updated, whereas in FBMC-MA the complexity is due to symbol demodulation and CFO compensation. We show that the separation of CFO update and CFO compensation operations reduce considerably the complexity in the high mobility scenario. Considering low CFO, we show that OFDMA outperform FBMC-MA and has lower complexity, whereas FBMC-MA works better than OFDMA for high CFO. On the other hand, for time-varying CFO we found that OFDMA is more robust to long update periods.

Acknowledgments

This work was partially funded by the Universidad Nacional del Sur PGI 24/K044 and PGI24/K043, the ANPCyT PICT-2008-0182 and PICT-2008-00104, the CONICET PIP 112-200801-01024 and PIP 2012-2014 GI, the Center of Excellence in Smart Radios and Wireless Research (SMARAD), and the Academy of Finland.

References

[1] Z. Cao, U. Tureli, Y.-D. Yao, Deterministic multiuser carrier-frequency offset estimation for interleaved OFDMA uplink, IEEE Trans. Commun. 52 (2004) 1585–1594.
[2] M.-O. Pun, M. Morelli, C.C.J. Kuo, Iterative detection and frequency synchronization for OFDMA uplink transmissions, IEEE Trans. Wirel. Commun. 6 (2007) 629–639.
[3] S. Barbarossa, M. Pompili, G.B. Giannakis, Channel-independent synchronization of orthogonal frequency division multiple access systems, IEEE J. Sel. Areas Commun. 20 (2002) 474–486.
[4] J. Krinock, M. Singh, M. Paff, V. Tien, A. Lonkar, L. Fun, C.-C. Lee, Comments on OFDMA ranging scheme described in IEEE 802.16ab-01/01r1, IEEE 802.16abc-01/24, 2001.
[5] P. Sun, M. Morelli, L. Zhang, Carrier frequency offset tracking in the IEEE 802.16e OFDMA uplink, IEEE Trans. Wirel. Commun. 9 (2010) 3613–3619.
[6] 3rd Generation Partnership Project (3GPP) Technical Specification Group Radio Access Network; Physical Layer Aspects for Evolved Universal Terrestrial Radio Access, UTRA, Release 7, 2006.
[7] IEEE Standard for Local and Metropolitan Area Networks Part 16: Air Interface for Broadband Wireless Access Systems, Amendment 3: Advanced Air Interface, IEEE Std. 802.16m, 2011.
[8] H. Saeedi-Sourck, Y. Wu, J.W.M. Bergmans, S. Sadri, B. Farhang-Boroujeny, Complexity and performance comparison of filter bank multicarrier and OFDM in uplink of multicarrier multiple access networks, IEEE Trans. Signal Process. 59 (2011) 1907–1912.
[9] P. Siohan, C. Siclet, N. Lacaille, Analysis and design of OFDM/OQAM systems based on filterbank theory, IEEE Trans. Signal Process. 50 (2002) 1170–1183.
[10] D. Huang, K.B. Letaief, An interference-cancellation scheme for carrier-frequency offsets correction in OFDMA systems, IEEE Trans. Commun. 53 (2005) 203–204.
[11] P. Sun, L. Zhang, Low complexity iterative interference cancelation for OFDMA uplink with carrier frequency offsets, in: Proc. IEEE 15th Asia-Pacific Conf. on Commun., 2009, pp. 390–393. http://dx.doi.org/10.1109/APCC.2009.5375611.
[12] Z. Cao, U. Tureli, Y.-D. Yao, Low-complexity orthogonal spectral signal construction for generalized OFDMA uplink with frequency synchronization errors, IEEE Trans. Veh. Technol. 56 (2007) 1143–1154.
[13] M.-O. Pun, M. Morelli, C.C.J. Kuo, Multi-Carrier Techniques For Broadband Wireless Communications: A Signal Processing Perspectives, Imperial College Press, London, UK, 2007.
[14] J. Choi, C. Lee, H.W. Jung, Y.H. Lee, Carrier frequency offset compensation for uplink of OFDM-FDMA systems, IEEE Commun. Lett. 4 (2000) 414–416.
[15] R. Fa, L. Zhang, R. Ramirez-Gutierrez, Blind carrier frequency offset tracking based on multiuser interference cancellation in OFDMA uplink systems, in: Proc. 18th European Wireless Conf., 2012, pp. 1–5.
[16] L. Kuang, J. Lu, Z. Ni, J. Zheng, Nonpilot-aided carrier frequency tracking for uplink OFDMA systems, in: Proc. IEEE International Conf. on Commun., volume 6, 2004, pp. 3193–3196. http://dx.doi.org/10.1109/ICC.2004.1313133.
[17] S. Talbot, B. Farhang-Boroujeny, Time-varying carrier offsets in mobile OFDM, IEEE Trans. Commun. 57 (2009) 2790–2798.
[18] LTE; evolved universal terrestrial radio access (E-UTRA); base station (BS) radio transmission and reception, 2012.
[19] H. Holma, A. Toskala, LTE for UMTS—OFDMA and SC-FDMA Based Radio Access, first ed., Wiley, 2009.
[20] Q. Bai, J. Nossek, On the effects of carrier frequency offset on cyclic prefix based OFDM and filter bank based multicarrier systems, in: Proc. IEEE 11th Signal Processing Advances in Wireless Commun., 2010, pp. 1–5. http://dx.doi.org/10.1109/SPAWC.2010.5670999.
[21] D. Petrovic, W. Rave, G. Fettweis, Effects of phase noise on OFDM systems with and without PLL: characterization and compensation, IEEE Trans. Commun. 55 (2007) 1607–1616.
[22] Q. Wang, C. Mehlführer, M. Rupp, Carrier frequency synchronization in the downlink of 3GPP LTE, in: Proc. IEEE 21st International Symposium Personal, Indoor Mobile Radio Commun., 2010, pp. 939–944. http://dx.doi.org/10.1109/PIMRC.2010.5671968.
[23] PHYDYAS Deliverable D5.1: Prototype Filter and Structure Optimization, Physical layer for Dynamic Access and Cognitive Radio, 2008.
[24] PHYDYAS Deliverable D3.1: Equalization and Demodulation in the Receiver (Single Antenna), Physical Layer for Dynamic Access and Cognitive Radio, 2009.
[25] Z. Cao, U. Tureli, Y.-D. Yao, Frequency synchronization for generalized OFDMA uplink, in: Proc. IEEE Global Telecommun. Conf., volume 2, 2004, pp. 1071–1075. http://dx.doi.org/10.1109/GLOCOM.2004.1378122.
[26] G.H. Golub, C.F.V. Loan, Matrix Computations, third ed., The Johns Hopkins Univ. Press, 1996.
[27] N.J. Fliege, Computational efficiency of modified DFT polyphase filter banks, in: Proc. 27th Asilomar Conf. Signals, Systems Computers, volume 2, 1993, pp. 1296–1300. http://dx.doi.org/10.1109/ACSSC.1993.342326.
[28] ITU-R, Guidelines for Evaluation of Radio Transmission Technologies for IMT-2000, Recommendation ITUR M1225, 93, 1997, pp. 148–56.

Gustavo J. González was born in Bahía Blanca, Argentina. He received the B.Sc. degree in 2007, and the Ph.D. degree in 2012 from Universidad Nacional del Sur (UNS), Bahía Blanca, Argentina. In 2007, he joined the undergraduate Department of Electrical and Computer Engineering at UNS. He is postdoctoral fellow of the Consejo Nacional de Investigaciones Científicas y Técnicas (CONICET) since 2012. His research interests include digital signal processing for wireless communications, in particular frequency synchronization, OFDM/A, and filter bank multicarrier.

Fernando H. Gregorio is from Bahía Blanca, Argentina. He received the B.Sc. degree from the Universidad Tecnologica Nacional (UTN), Bahía Blanca, Argentina in 1999, the M.Sc. degree in electrical engineering from the Universidad Nacional del Sur (UNS), Bahía Blanca in 2003 and the D.Sc. (electrical engineering) degree from the Signal Processing Laboratory, Helsinki University of Technology (TKK), Espoo, Finland, in 2007. He is currently a professor in the Department of Electrical and Computer Engineering at UNS and researcher of the Consejo Nacional de Investigaciones Científicas y Técnicas (CONICET) of Argentina. His research interests include radio frequency impairments in MIMO–OFDM systems and multiuser communications.

Juan Cousseau was born in Mar del Plata, Argentina. He received the B.Sc from the Universidad Nacional del Sur (UNS), Bahia Blanca, Argentina, in 1983, the M.Sc. degree from COPPE/Universidade Federal do Rio de Janeiro (UFRJ), Brazil, in 1989, and the Ph.D. from COPPE/UFRJ, in 1993, all in electrical engineering.

Since 1984, he has been with the undergraduate Department of Electrical and Computer Engineering at UNS. He has also been with the graduate Program at the same university since 1994. He is a Senior researcher of the Consejo Nacional de Investigaciones Científicas y Técnicas (CONICET) of Argentina. He has been involved in scientific and industry projects with research groups from Argentina, Brazil, Spain, USA and Finland. He is coordinator of the Signal Processing and Communication Laboratory (LaPSyC) at UNS. He is Senior member of the IEEE. He was IEEE Circuits and Systems Chair of the Argentine Chapter, from 1997 to 2000, and member of the Executive Committee of the IEEE Circuits and Systems Society during 2000/2001 (Vicepresident for Region 9). He participates of the IEEE Signal Processing Society Distinguished Lecturer Program 2006. He is actually Director of the Municipal Agency of Science and Technology of Bahía Blanca city. His research interests are related to adaptive and statistical signal processing with application to modern broadband wireless communications.

Risto Wichman received his M.Sc. and D.Sc. (Tech) degrees in digital signal processing from Tampere University of Technology, Tampere, Finland, in 1990 and 1995, respectively. From 1995 to 2001, he worked at Nokia Research Center as a senior research engineer. In 2002, he joined Department of Signal Processing and Acoustics, Aalto University School of Electrical Engineering, Finland, where he is a full professor since 2008. His research interests include digital signal processing for wireless communications systems.

Stefan Werner received the M.Sc. degree in electrical engineering from the Royal Institute of Technology (KTH), Stockholm, Sweden, in 1998 and the D.Sc. (electrical engineering) degree (with honors) from the Signal Processing Laboratory, Helsinki University of Technology (TKK), Espoo, Finland, in 2002. He is currently an Academy Research Fellow in the Department of Signal Processing and Acoustics, Aalto University, Finland, where he is also appointed as a Docent. His research interests include adaptive signal processing, signal processing for communications, and statistical signal processing. He is a member of the editorial board for EURASIP's Signal Processing journal.